The Mechanism of the Reaction between t-Butyl Hydroperoxide and 5,10,15,20-Tetra(*N*-methyl-4-pyridyl)porphyrinatoiron(III) Pentachloride in Aqueous Solution

John R. Lindsay Smith * and Russell J. Lower
Department of Chemistry, University of York, York YO1 5DD, UK

The kinetics of the reaction of t-butyl hydroperoxide with 5,10,15,20-tetra(*N*-methyl-4-pyridyl)-porphyrinatoiron(III) pentachloride in aqueous solution have been investigated using 2,2′-azinobis(3-ethylbenzthiazoline-6-sulphonate) (ABTS) as a one-electron trap for the active oxidants. The reaction shows first-order dependence on the concentration of the hydroperoxide and of the iron(III) porphyrin. The measured second-order rate constants (k_2) increase linearly with the ionic strength of the medium. However, large changes in the concentrations of the buffers, while maintaining a constant ionic strength, have only small effects on k_2. The log k_2/pH profile of the reaction, from pH 4–10.2, is complex and in acidic solution the k_2 values show a dependence on the nature of the buffering species.

The products from the catalysed reaction of t-butyl hydroperoxide in the presence and absence of ABTS have been determined and the accountability of the oxidant is excellent. With ABTS present the major product is t-butyl alcohol whilst in its absence the yield of this alcohol is very small and acetone, methanol, formaldehyde and t-butylmethyl peroxide predominate. The product distribution is not dependent on the pH of the reaction medium but it is sensitive to the presence of dioxygen. In particular, the yields of methanol and t-butylmethyl peroxide are highest under anaerobic conditions whereas in air these yields decrease with a concomitant increase in formaldehyde.

The mechanisms of peroxide bond cleavage by the iron(III) porphyrin are discussed. The results are shown to be in agreement with a homolytic process generating an oxoiron(IV) porphyrin and a t-butoxyl radical rather than a heterolytic step to give an oxoiron(IV) porphyrin π radical cation and t-butyl alcohol.

A thorough understanding of the reactions of hydroperoxides with iron(III) porphyrins is a prerequisite for a full appreciation of the mechanisms of the peroxidases,[1] catalases[2] and the 'peroxide shunt' pathway of cytochrome P450 monooxygenases.[3] It would also help identify the role of haem compounds in pathologies associated with hydroperoxide metabolism.[4] In this respect much recent work has concentrated on the mechanisms of the initial steps in the reactions of alkyl hydroperoxides with synthetic metalloporphyrins. However, there is no general agreement on the mechanism of the cleavage of the O–O bond. Traylor and co-workers[5] propose a heterolytic two-electron transfer from the iron to the peroxide, analogous to the mechanism of horse radish peroxidase [reaction (1)]. By contrast, with Bruice and co-workers, we have provided evidence that this step is homolytic [reaction (2)].[6] Support for the latter mechanism comes from the ^{1}H NMR spectroscopic studies by Balch's research group on alkylperoxoiron porphyrins.[7]

The products from iron(III) porphyrin-catalysed oxidations of organic compounds by hydroperoxides in aprotic solvents have generally been accounted for by assuming that the active oxidant is an alkoxyl radical from homolysis of t-butyl hydroperoxide [reaction (2)] rather than the oxoiron(IV) porphyrin π radical cation in reaction (1).[8] The former mechanism has been confirmed in a recent thorough investigation by Labeque and Marnett for the reaction of tetraphenylporphyrinatoiron(III) chloride with 10-hydroperoxyoctadeca-8,12-dienoic acid.[9] However, the mechanism of these reactions may be modified to favour two-electron reduction of the peroxide by using good electron donor axial ligands, such as imidazole, which can stabilise the high valent oxo-iron intermediates.[9,10] Alternatively, improving the leaving group property of the anions formed by heterolysis of the peroxide can also lead to the two-electron process being preferred. The latter can be achieved using hydroperoxides substituted with electron-withdrawing groups or, more effectively by using peroxy acids.[11]

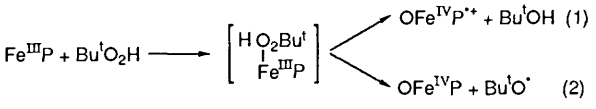

In our recent collaborative work with Bruice and his co-workers we have made extensive studies of the reaction of the sterically hindered, water-soluble, anionic 5,10,15,20-tetra(2,6-dimethyl-3-sulphonatophenyl)porphyrinatoiron(III) [Fe^{III}TDMSPP]† in aqueous solution.[6a,b] This catalyst was chosen to eliminate complications arising from aggregation and μ-oxo-dimer formation.[12] In this paper we report our studies on the reaction of t-butyl hydroperoxide with the unhindered cationic 5,10,15,20-tetra(*N*-methyl-4-pyridyl)porphyrinatoiron(III) [Fe^{III}T4MPyP].

Results

Kinetic Studies

*The kinetics of the reaction between t-butyl hydroperoxide and 5,10,15,20-Tetra(*N*-methyl-4-pyridyl)porphyrinatoiron(III) pentachloride.* These have been studied in aqueous solution at 30 °C at constant ionic strength [μ = 0.20 mol dm^{-3} with $NaNO_3$ using the one-electron trap diammonium 2,2′-azino-

† *Abbreviations:* Fe^{III}TDMSPP, 5,10,15,20-tetra(2,6-dimethyl-3-sulphonatophenyl)porphyrinatoiron(III); Fe^{III}T4MPyP, 5,10,15,20-tetra(*N*-methyl-4-pyridyl)porphyrinatoiron(III); Fe^{III}P, iron(III) porphyrin; OFe^{IV}P, oxoiron(IV) porphyrin; OFe^{IV}P$^{+\bullet}$, oxoiron(IV) porphyrin π radical cation; Fe^{II}P iron(II) porphyrin; ABTS, diammonium 2,2′-azinobis(3-ethylbenzthiazoline-6-sulphonate).

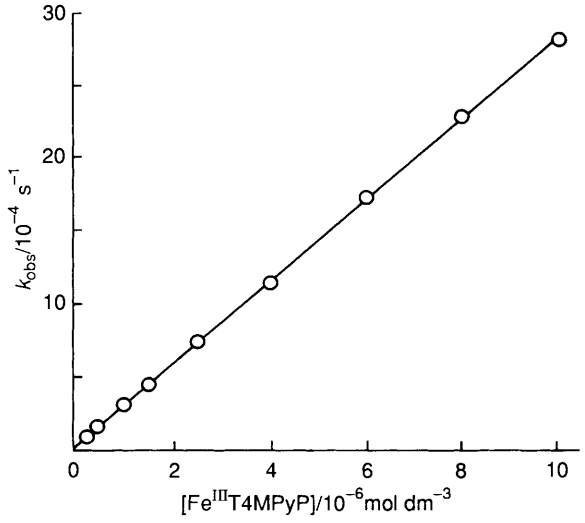

Fig. 1 Dependence of pseudo-first-order rate constant for formation of ABTS$^{\bullet+}$ on the concentration of Fe^{III}T4MPyP. Bu^{t}O$_2$H, 6.25 × 10^{-5} mol dm^{-3}; ABTS, 9.38 × 10^{-3} mol dm^{-3}; 0.1 mol dm^{-3} borate buffer, pH 9.16, (μ = 0.20 mol dm^{-3} with NaNO$_3$) at 30 °C.

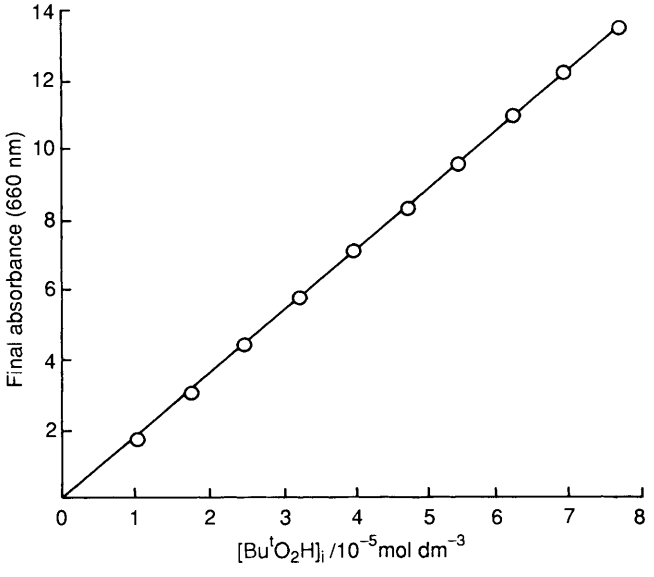

Fig. 2 Dependence of the final absorbance at 660 nm on the initial concentration of Bu^{t}O$_2$H. Fe^{III}T4MPyP, 2.5 × 10^{-6} mol dm^{-3}; ABTS, 9.38 × 10^{-3} mol dm^{-3}, 0.1 mol dm^{-3} borate buffer, pH 9.16 (μ = 0.20 mol dm^{-3} with NaNO$_3$) at 30 °C.

bis(3-ethylbenzthiazoline-6-sulphonate), ABTS]. As reported in previous studies,[6a] ABTS is an efficient trap for both high valent oxo-iron porphyrins and alkoxyl radicals. It is oxidised to the blue–green radical cation ABTS$^{\bullet+}$ (λ_{max}660 nm, ε_{660} 1200 m^2 mol^{-1}) which in the presence of a large excess of ABTS is stable towards further oxidation to ABTS^{2+}.

The kinetic system was characterised in 0.1 mol dm^{-3} aqueous borate buffer, pH 9.16. A blank experiment showed that in the absence of the iron(III) porphyrin the ABTS is not oxidised by Bu^{t}O$_2$H. Kinetic studies used (0.25–10) × 10^{-6} mol dm^{-3} Fe^{III}T4MPyP with 6.25 × 10^{-5} mol dm^{-3} Bu^{t}O$_2$H and 9.38 × 10^{-3} mol dm^{-3} ABTS. Under these conditions, the formation of ABTS$^{\bullet+}$ follows first-order kinetics and the observed pseudo-first-order rate constants, k_{obs}, vary linearly with [Fe^{III}T4MPyP] (Fig. 1). Changing the large excess of ABTS from 1500 to 5000-fold while keeping other reactant concentrations constant has no effect on k_{obs}. However, changing the initial concentration of the Bu^{t}O$_2$H influences the final yield of ABTS$^{\bullet+}$ and the rate of the reaction. A plot of the final absorbances at 660 nm *vs.*

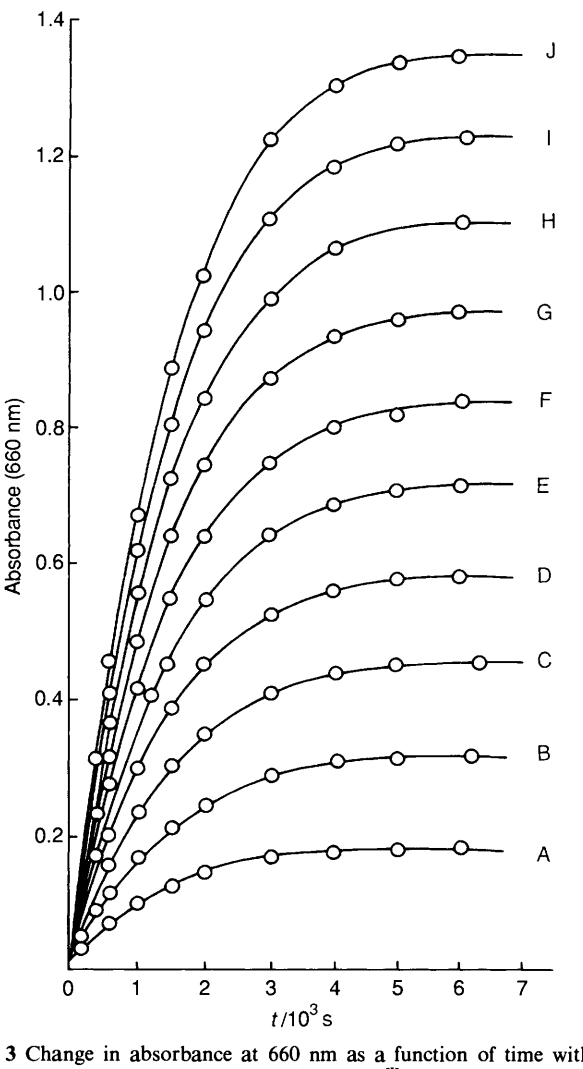

Fig. 3 Change in absorbance at 660 nm as a function of time with different initial concentrations of Bu^{t}O$_2$H. Fe^{III}T4MPyP, 2.5 × 10^{-6} mol dm^{-3}; ABTS, 9.38 × 10^{-3} mol dm^{-3}; 0.1 mol dm^{-3} borate buffer, pH 9.16, (μ = 0.20 mol dm^{-3} with NaNO$_3$) at 30 °C. [Bu^{t}O$_2$H]$_i$/10^{-5} mol dm^{-3}: A = 1.00; B = 1.75; C = 2.50; D = 3.25; E = 4.00; F = 4.75; G = 5.50; H = 6.25; I = 7.00; J = 7.75.

[Bu^{t}O$_2$H]$_i$ (Fig. 2) shows the linear relationship between ABTS$^{\bullet+}$ yield and initial oxidant concentration. Assuming that Bu^{t}O$_2$H generates 2 equiv. of ABTS$^{\bullet+}$, the slope of Fig. 2 gives a yield of ABTS$^{\bullet+}$ of 72%.

The change in A_{660} *vs.* time for different [Bu^{t}O$_2$H]$_i$ provides initial rates for the formation of ABTS$^{\bullet+}$ (Fig. 3) which are linearly dependent on [Bu^{t}O$_2$H]$_i$ (Fig. 4 has a slope of 8.20 × 10^{-4} s^{-1}). When allowance has been made for the 72% overall yield of ABTS$^{\bullet+}$, these data give a pseudo-first-order rate constant for reaction with Bu^{t}O$_2$H of 5.69 × 10^{-4} s^{-1}. This value compares well with the average value of k_{obs} = 6.90 × 10^{-4} s^{-1} from first-order analyses for the rates of ABTS$^{\bullet+}$ formation.

The results above show that the reactions follow the rate law, d[ABTS$^{\bullet+}$]/dt = k_2[Fe^{III}T4MPyP][Bu^{t}O$_2$H], where k_{obs} = k_2[Fe^{III}T4MPyP].

The dependence of the reaction rate on the ionic strength of the medium. This was investigated by varying the sodium nitrate concentration. The second-order rate constant, k_2, was found to increase linearly with ionic strength, in the range μ = 0.075–0.5 mol dm^{-3} from 153–457 dm^3 mol^{-1} s^{-1} (Fig. 5).

The pH dependence of the second-order rate constant, k_2. This was investigated over the range pH 4.00–10.20. These studies were not carried out over a wider range since in more acidic or

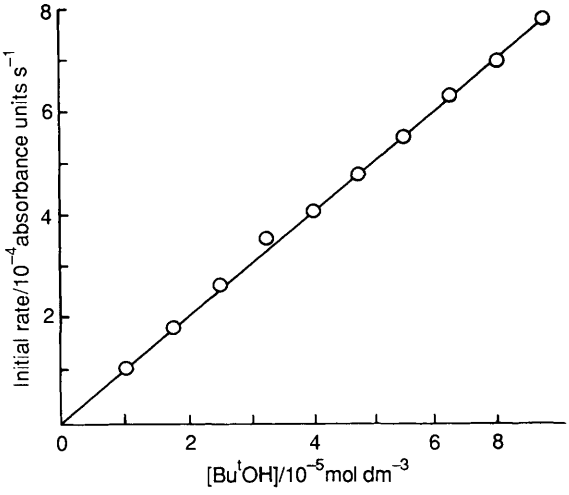

Fig. 4 Dependence of the initial slopes from plots of change in absorbance at 660 nm *vs.* time on initial Bu^tO_2H concentration. Fe^{III}T4MPyP, 2.5 × 10^{-6} mol dm^{-3}; ABTS, 9.38 × 10^{-3} mol dm^{-3}, 0.1 mol dm^{-3} borate buffer, pH 9.16; (μ = 0.20 mol dm^{-3} with $NaNO_3$) at 30 °C.

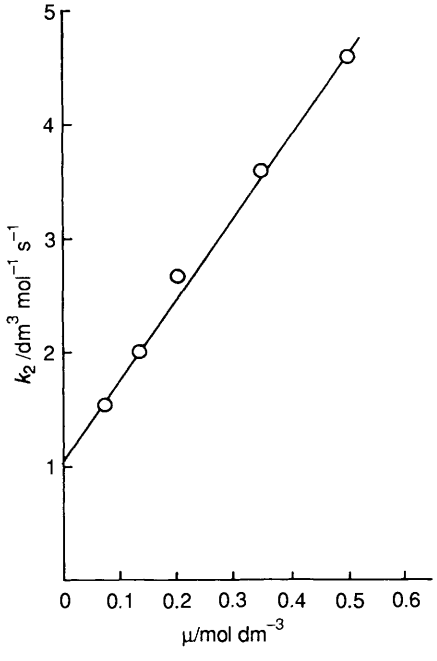

Fig. 5 Dependence of the second-order rate constant for formation of $ABTS^{\bullet+}$ on the ionic strength of the reaction medium. Fe^{III}T4MPyP, 5.0 × 10^{-6} mol dm^{-3}; Bu^tO_2H, 5.0 × 10^{-5} mol dm^{-3}; ABTS, 7.50 × 10^{-3} mol dm^{-3}; 0.1 mol dm^{-3} borate buffer, pH 9.16 at 30 °C.

basic solution the kinetics are complicated by other reactions of ABTS and $ABTS^{\bullet+}$, respectively.[6a] The buffers employed (with their pH ranges) were as follows: acetic acid–acetate (4.00–5.75), hydrogen phthalate–phthalate dianion (4.35–6.45), dihydrogen phosphate–monohydrogen phosphate (6.00–7.80) and trihydrogen borate–dihydrogen borate (8.10–10.20). Fig. 6 shows how the log of the second-order rate constant for the reaction of Fe^{III}T4MPyP with Bu^tO_2H in the presence of excess of ABTS changes with the pH of the reaction mixture. This pH–rate constant profile bears a strong resemblance to that obtained, using the same experimental conditions, from the sterically hindered anionic Fe^{III}TDMSPP (data included in Fig. 6 for comparison).[6a] Thus, the magnitude of the rate constants and the positions of the inflexions with both catalysts are comparable. However, in this study we observed a buffer-dependent dis-

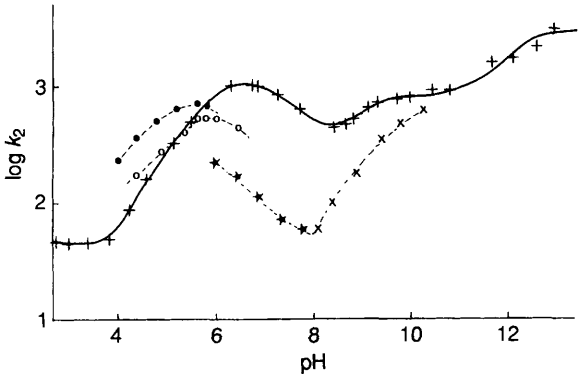

Fig. 6 Log values of the second-order rate constant *vs.* the pH of the reaction mixture for reaction of Fe^{III}T4MPyP with Bu^tO_2H (– – –). ABTS, 7.50 × 10^{-3} mol dm^{-3}; (μ = 0.20 mol dm^{-3} with $NaNO_3$) at 30 °C. (×) borate buffer, (*) phosphate buffer, (○) phthalate buffer, (●) acetate buffer. Fe^{III}TDMSPP with Bu^tO_2H (——). ABTS, 1 × 10^{-2} mol dm^{-3}; (μ = 0.22 mol dm^{-3} with $NaNO_3$) at 30 °C.[6a]

continuity in the acidic region that was not found with the anionic iron(III) porphyrin.

The dependence of the second-order rate constant on the buffer concentration. This was examined with each of the buffers. For the phosphate and borate buffer systems, at pH 6.86 and 9.16, respectively, a tenfold increase in the buffer concentration has a small accelerating effect; the second-order rate constant increased by <20%. With acetate and phthalate at pH 5.0 the same change in the buffer concentration results in a small linear decrease in k_2 of 30 and 40%, respectively.

Product Studies

The products from the reaction of Fe^{III}T4MPyP *with* Bu^tO_2H. These have been determined under a wide variety of conditions. With reactions in the presence of ABTS the yield of $ABTS^{\bullet+}$ was obtained from the value of A_{660} at the end of each of the kinetic experiments and shown to decrease slightly with increasing pH of the reaction mixture (yield 69% and 79% at pH 10.2 and 4.0, respectively). There is also a small but measurable decrease in the yield of $ABTS^{\bullet+}$ when acetate buffer is replaced by phthalate buffer.

All the products from Bu^tO_2H, except formaldehyde, were analysed directly by GC. To increase the yields of the products these reactions were carried out with a higher oxidant:catalyst ratio (500:1) than was used in the kinetic studies. Formaldehyde was determined colorimetrically by Nash's method.[13] The product yields in Table 1 can be considered under four regimes: (i) unstirred reactions in air in the presence of ABTS, (ii) stirred reactions in air in the absence of ABTS, (iii) unstirred reactions in air in the absence of ABTS and (iv) unstirred reactions under nitrogen in the absence of ABTS.

Under each of the four regimes the product balances are excellent and no major product remains undetected. Furthermore, the product distributions show no significant dependence on the pH of the reaction mixture.

With ABTS present in the reaction the major product from Bu^tO_2H is Bu^tOH. The remainder of the oxidant is recovered as methanol and acetone. Under these conditions the visible absorbance of $ABTS^{\bullet+}$ makes it impossible to make the colorimetric estimation of the yield of formaldehyde. When the ABTS is omitted from the reaction, acetone (>70%) replaces Bu^tOH as the major product; the latter under these conditions is only present in small amounts. Other important products are methanol, formaldehyde and t-butylmethyl peroxide. Di-t-butyl peroxide was only present in trace amounts.

Comparing the reactions in the presence and absence of air reveals some important differences in the product distribution.

Table 1 Percentage yields of products from the reaction of Bu^tO_2H with $Fe^{III}T4MPyP$ in aqueous solution: $Fe^{III}T4MPyP$, 5.0×10^{-6} mol dm^{-3}; Bu^tO_2H, 2.5×10^{-3} mol dm^{-3}; borate buffer, 0.1 mol dm^{-3}, pH = 9.2, μ = 0.20 mol dm^{-3} with $NaNO_3$

Reaction conditions	Yields of products (%)[a]					Carbon balance (%)	
	Bu^tOH	Me_2CO	MeOH	HCHO	Bu^tO_2Me	$(C_3 + C_4)^b$	$(C_1 + C_4)^b$
ABTS in air unstirred	98	4	3	n.d.[c]	—	102	—
No ABTS in air stirred	6	79	15	56	12	97	101
No ABTS in air unstirred	4	77	30	26	19	100	98
No ABTS under N_2 unstirred	1	70	35	3	30	101	99

[a] Based on oxidant, small quantities of methane and ethane were also detected (see Table 2). [b] $(C_3 + C_4)$ is the sum of the percentage yields of Bu^tOH, Me_2CO and Bu^tO_2Me, $(C_1 + C_4)$ is the sum of the percentage yields of Bu^tOH, MeOH, HCHO and 2 × Bu^tO_2Me. [c] Interference from $ABTS^{\bullet+}$ made colorimetric determination of HCHO impossible.

Table 2 The percentage yields of methane and ethane from the reaction of Bu^tO_2H with $Fe^{III}T4MPyP$ in aqueous solution: $Fe^{III}T4MPyP$, 5×10^{-6} mol dm^{-3}; borate buffer, 0.1 mol dm^{-3}, pH = 9.2

Reaction conditions		Yield of products (%)[a]	
[Oxidant]/mol dm^{-3}	Air/Nitrogen[b]	Methane	Ethane
Bu^tO_2H (5×10^{-4})	N_2	0.17	0.20
Bu^tO_2H (2.5×10^{-3})	N_2	0.27	0.13
Bu^tO_2H (1.25×10^{-2})	N_2	0.51	0.05
Bu^tO_2D (2.5×10^{-3})	N_2	0.08[c]	0.20
Bu^tO_2H (2.5×10^{-3})	Air	0.16	0.05
Bu^tO_2H (2.5×10^{-3})	Air[d]	0.01	trace

[a] Based on oxidant. [b] Reaction mixtures unstirred. [c] CH_4 (85%), CH_3D (15%). [d] Reaction mixtures stirred.

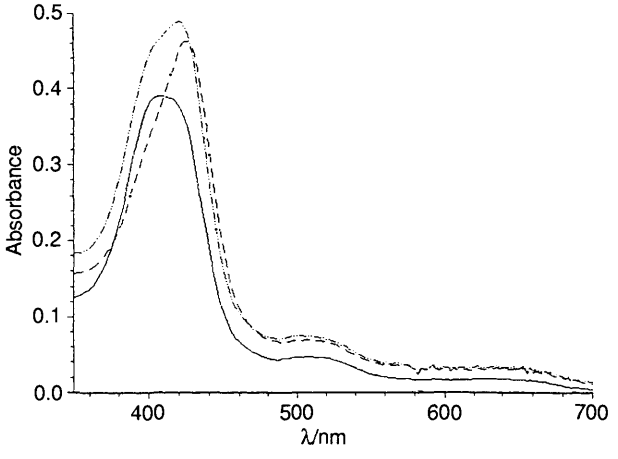

Fig. 7 UV-vis. spectra of $Fe^{III}T4MPyP$ in aqueous solution at pH 4.0, 30 °C. 0.05 mol dm^{-3} buffers, acetate (———), phthalate (– – –) and succinate (– • • – • • –)

On changing from anaerobic to unstirred aerobic conditions there is a dramatic increase in the yield of formaldehyde, smaller but significant increases in t-butyl alcohol and acetone and concomitant decreases in methanol and t-butylmethyl peroxide. Stirring the reactions carried out in air emphasises these changes in yields.

Although the product balances above are excellent we investigated whether some of the Bu^tO_2H was converted into methane and ethane. GC and GC–MS analyses of the headspace gas above reactions showed the presence of both products in low yields in all the reactions (Table 2). Reactions under nitrogen showed the highest yields of these hydrocarbons. Increasing the amount of hydroperoxide in the reaction mixture led to an increase in methane at the expense of ethane. When the reaction under nitrogen was repeated with Bu^tO_2D, prepared by H/D exchange of Bu^tO_2H in D_2O, the methane was found to be 15% monodeuteriated and the ratio of methane to

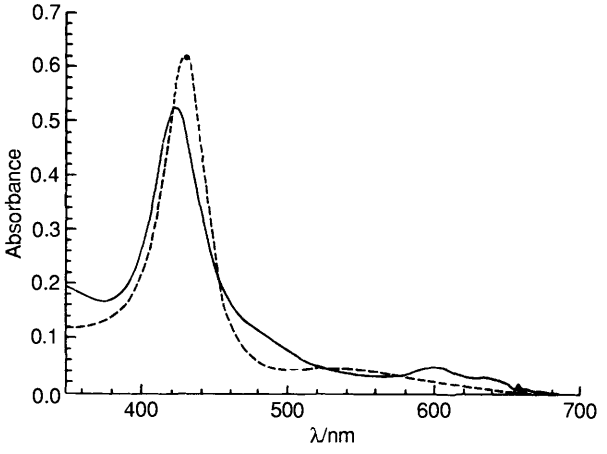

Fig. 8 UV–VIS spectrum of $Fe^{III}T4MPyP$ (———) before and (– – –) 60 s after the addition of Bu^tO_2H. $Fe^{III}T4MPyP$, 5×10^{-6} mol dm^{-3}; Bu^tO_2H, 5×10^{-5} mol dm^{-3}; 0.1 mol dm^{-3} borate buffer, pH 9.16; (μ = 0.20 mol dm^{-3} with $NaNO_3$) at 30 °C.

ethane changed from 2.1 for Bu^tO_2H to 0.4 for the deuterio analogue.

UV–VIS spectra of $Fe^{III}T4MPyP$ *in aqueous buffers at pH* 4.0. The UV-VIS spectrum of $Fe^{III}T4MPyP$ was recorded at pH 4.0 in a selection of 0.05 mol dm^{-3} carboxylic acid–carboxylate buffering systems (Fig. 7). The concentrations of the catalyst and the buffer were typical of those used for the kinetic studies. The Soret absorptions in the spectra show that the porphyrin species present in the mixtures are dependent on the nature of the buffer.

UV–VIS spectroscopic studies of the iron porphyrin species in the reaction of Bu^tO_2H *with* $Fe^{III}T4MPyP$. The green-brown aqueous solutions of $Fe^{III}T4MPyP$ at pH 9.2 become red on addition of >1 mol equiv. of Bu^tO_2H in air. The UV–VIS spectra of the starting porphyrin and the red species are shown in Fig. 8. At room temperature the red colour decays slowly with time and the UV–VIS spectrum returns to that of the starting porphyrin. Large excesses of the oxidant lead to some bleaching of the $Fe^{III}T4MPyP$; typically a 500-fold excess of Bu^tO_2H produces 15% loss of catalyst.

When the reactions are carried out under nitrogen, with a 500-fold excess of Bu^tO_2H, the almost complete conversion of the iron(III) porphyrin into the red intermediate followed by its decay back to $Fe^{III}T4MPyP$ is again observed. However, with only a ten-fold excess of oxidant, UV–VIS spectral simulation shows that <15% of the red intermediate is formed. Under the latter conditions the dominant species is $Fe^{III}T4MPyP$ and no evidence for $Fe^{II}T4MPyP$ (Soret λ_{max} 448 mm) was obtained. When the reaction with a tenfold excess of oxidant is repeated in the presence of carbon monoxide the initially formed red intermediate decays with time and is completely converted into the carbon monoxide adduct of $Fe^{II}T4MPyP$ (Fig. 9). The

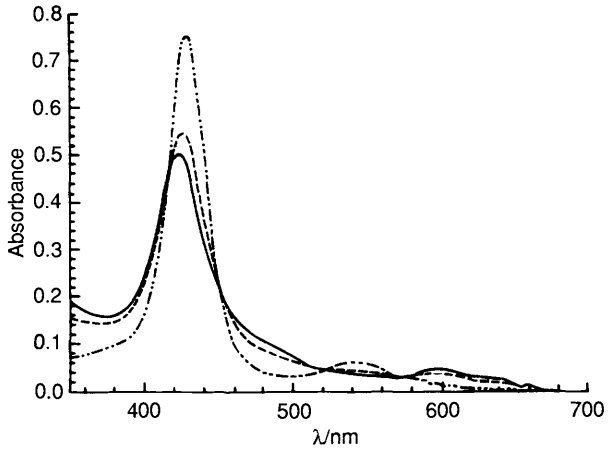

Fig. 9 UV–VIS spectrum of the reaction of $Fe^{III}T4MPyP$ with Bu^tO_2H under anaerobic conditions in the presence of CO, (———) before addition of Bu^tO_2H, and (– – –) 30 s and (–••–••–) 6 × 10^3 s after addition. $Fe^{III}T4MPyP$, 5 × 10^{-6} mol dm^{-3}; Bu^tO_2H, 5 × 10^{-5} mol dm^{-3}; 0.1 mol dm^{-3} borate buffer, pH 9.16; (μ = 0.20 mol dm^{-3} with $NaNO_3$) at 30 °C.

Table 3 The iron porphyrin species present during the reaction of $Fe^{III}T4MPyP$ with Bu^tO_2H in an atmosphere of nitrogen and carbon monoxide. $Fe^{III}T4MPyP$, 5 × 10^{-6} mol dm^{-3}; Bu^tO_2H, 5 × 10^{-5} mol dm^{-3}; borate buffer, 0.1 mol dm^{-3}, pH 9.2

	Distribution of iron porphyrins (%)[a]		
Time/min	$Fe^{III}T4MPyP$	$OFe^{IV}T4MPyP$	$(CO)Fe^{II}T4MPyP$
0	100	0	0
0.5	58	21	15
100	0	0	100

[a] Distributions of iron porphyrins were obtained from computer simulation of UV–VIS spectra of reaction mixtures.

relative proportions of the oxoiron(IV), iron(III) and (CO)iron(II) porphyrins have been obtained by simulation of the UV–VIS spectra recorded at different times during the course of the reaction (Table 3).

Discussion

The sterically hindered anionic porphyrin, $Fe^{III}TDMSPP$, was selected for our previous investigations of the catalysed decompositions of Bu^tO_2H to eliminate possible complications from μ-oxo-dimer formation and aggregation. We have now extended these studies to the unhindered cationic $Fe^{III}T4MPyP$. We find that the product distribution and the kinetic behaviour of the two porphyrins with Bu^tO_2H, despite differences in charge and steric hindrance in the catalysts, are remarkably similar.

Kinetic Studies on the $Fe^{III}T4MPyP$*-catalysed Decomposition of* Bu^tO_2H.—In the presence of a large excess of ABTS the catalysed decomposition of Bu^tO_2H is first-order in both the $[Fe^{III}P]_i$ and $[Bu^tO_2H]_i$ and is independent of $[ABTS]_i$.

The observed second-order kinetics, however, cannot be used to distinguish between an initial one- or two-electron reduction of Bu^tO_2H by $Fe^{III}T4MPyP$ [reactions (2) and (1), respectively]. ABTS rapidly traps the two oxidising equivalents whether they are present as $OFe^{IV}P$ with the t-butoxyl radical or as $OFe^{IV}P^{\bullet+}$ [reaction (3)] and the observed second-order rate constant could be for either reaction (1) or (2).

The pH of the reaction mixture will control the axial ligands on the iron(III) porphyrin which will, in turn, influence the activity of the catalyst. Furthermore, it is well known that in basic solution unhindered hydroxyiron(III) porphyrins are prone to form μ-oxo dimers.[14] There have been a number of

$$\left.\begin{array}{l} OFe^{IV}P + Bu^tO^{\bullet} \\ \text{or} \\ OFe^{IV}P^{+\bullet} + Bu^tOH \end{array}\right\} + 2ABTS \longrightarrow 2ABTS^{\bullet+} + Fe^{III}P + Bu^tOH \quad (3)$$

studies on $Fe^{III}T4MPyP$ in aqueous solution which have attempted to identify the porphyrin species present at different pHs.[15] A recent very thorough examination by Buckingham and co-workers [15d] concludes that there are two pH dependent monomer–monomer equilibria and in basic solution there is one concentration dependent monomer–dimer equilibrium (Scheme 1). Calculations based on these data suggest that at all the pH values and concentrations used in this study the catalyst would have been present as monomers. Consequently in this respect, $Fe^{III}T4MPyP$ should be no different to the sterically hindered $Fe^{III}TDMSPP$ used previously.[6a] This is in agreement with our results, since the rate of the catalysed decomposition of Bu^tO_2H shows a good first-order dependence on $[Fe^{III}P]_i$ over a 40-fold range of catalyst concentration. If the solutions had been mixtures of monomers and dimers this simple behaviour would not have been expected.

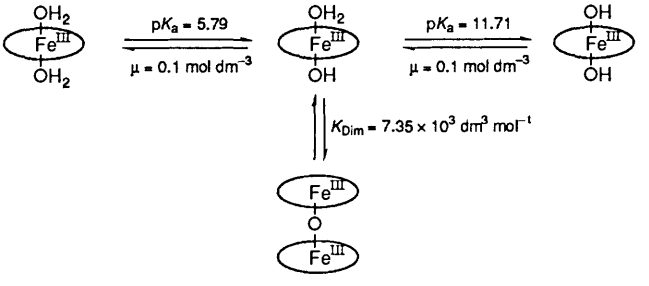

Scheme 1

The reactions with $Fe^{III}T4MPyP$, unlike those of $Fe^{III}TDMSPP$, are sensitive to changes in the ionic strength of the medium (Fig. 5). Thus, a 6.7-fold increase in ionic strength produces a threefold increase in the second-order rate constant. Goff and Morgan [14b] used magnetic moment measurements (Evans method) to show that increasing ionic strength leads to increased μ-oxo dimer formation with $Fe^{III}T4MPyP$. However, they used significantly more concentrated solutions than in this study ($\geqslant 5 \times 10^{-3}$ as opposed to 5 × 10^{-6} mol dm^{-3}) and this would have favoured dimerisation. We do not believe that, even at the highest ionic strength (μ = 0.5 mol dm^{-3}) significant amounts of μ-oxo dimers were present in this study. Furthermore, we would expect dimer formation to lead to a decreased rather than an increased rate of reaction. The cause of this salt effect remains unresolved.

Although the kinetic rate law and the product distributions for the reaction of Bu^tO_2H with $Fe^{III}T4MPyP$ are unaffected by the pH of the reaction medium, the second-order rate constant has a complex dependence on pH. The overall shape of the $\log k_2$ *vs.* pH profile is very similar to that obtained from the hindered anionic $Fe^{III}TDMSPP$ (Fig. 6).[6a] However, for $Fe^{III}T4MPyP$ there is a buffer-dependent dislocation in the acidic pH region. We interpret this as arising from ligation of the buffer to the iron(III) porphyrin to produce species with differing catalytic activities. The buffer dependence of the λ_{max} value of the Soret band of the catalyst at pH 4.0 supports this explanation since it shows that even at 0.05 mol dm^{-3} concentration the buffer can compete effectively with water for the axial position of the iron(III) porphyrin. The absence of this effect with $Fe^{III}TDMSPP$ may be due to steric hindrance and charge repulsion making it a less favourable process.

We have not attempted to fit the log k_2 *vs.* pH data to an empirical equation in the manner described previously.[6a] How-

ever, a minimum of three pK dependent equilibria are needed to account for the results, the pK_a values of which are *ca.* 5.0, 6.5 and 9.2. The identity of the iron(III) porphyrin species that give rise to these equilibria are under investigation.

The Reaction of Fe^{III}T4MPyP *with* Bu^tO_2H *in the Presence of ABTS.*—Since the kinetic studies do not provide evidence for the mechanism of the cleavage of the O–O bond of Bu^tO_2H by Fe^{III}T4MPyP, we have carried out a detailed examination of the products derived from the hydroperoxide. With the sterically hindered anionic Fe^{III}TDMSPP we accounted for the observed kinetics and products in terms of an initial ligation of the Bu^tO_2H followed by homolysis of the O–O bond to give the $Bu^tO^\bullet$ radical and an iron(IV) porphyrin [reaction (2)]. With a large excess of ABTS the majority of these intermediates are reductively trapped [reactions (3)].[6a] This mechanistic pathway can also account for the predominant formation of Bu^tOH (98%) and $ABTS^{\bullet+}$ (74 ± 5%) using the cationic porphyrin employed in the present study. The remainder of the products from Bu^tO_2H arise from a small proportion of the Bu^tO radicals fragmenting[16] before they are trapped by ABTS [reaction (4)]. The oxidation of the methyl radicals [reactions (5) and (6)] are known to be extremely rapid reactions. The rate of the former reaction has been measured in pulse radiolytic studies[17] and the latter is an important step in the oxygen-rebound mechanism for the hydroxylation of unactivated C–H bonds by oxo-iron(IV) porphyrin π radical cations[18] and by cytochrome P450 mono-oxygenases.[19] However, the products might equally well

$$Bu^tO^\bullet \longrightarrow Me^\bullet + Me_2CO \quad (4)$$

$$Me^\bullet + Fe^{III}P \xrightarrow{H_2O} MeOH + Fe^{II}P \quad (5)$$

$$Me^\bullet + OFe^{IV}P \longrightarrow MeOH + Fe^{III}P \quad (6)$$

arise from a two-electron heterolytic cleavage [reaction (1)] with ABTS trapping the oxoiron(IV) porphyrin π radical cation [reaction (3)]. The small amount of radical derived products would be formed by the competitive reaction of the oxoiron(IV) porphyrin π radical cation with Bu^tO_2H [reaction (7)]. This argument is analogous to that proposed by Traylor and co-workers[20] for the reaction of hydroperoxides with iron(III) porphyrins in the presence of norbornene. They suggest that the alkene is only epoxidised by the oxoiron(IV) porphyrin π radical cation when the hydroperoxide concentration is sufficiently low for the alkene to compete effectively with Bu^tO_2H for the active oxidant.

$$Bu^tO_2H + OFe^{IV}P^{\bullet+} \longrightarrow Bu^tO_2^\bullet + OFe^{IV}P \quad (7)$$

Reaction of Fe^{III}T4MPyP *with* Bu^tO_2H *in the Absence of ABTS.*—When the reactions are carried out in the absence of ABTS the major product is acetone arising from fragmentation of the t-butoxyl radicals [reaction (4)][16] and t-butyl alcohol is a minor product (Table 1). The methyl radical from reaction (4) reacts further to give t-butylmethyl peroxide and the one-carbon products methanol and formaldehyde. As predicted by reaction (4), the sum of the yields of these products for the reactions carried out under each set of conditions is found to equal that of acetone (Table 1). This excellent product balance shows that all the major products from the methyl radical in these reactions have been accounted for. The very small proportion that ends up as methane and ethane, in this respect is not significant. The alternative pathways available for reaction of the methyl radical are discussed below.

The Fate of the $Bu^tO_2^\bullet$ *Radical and the Origin of* Bu^tO_2Me.—Our ESR spectroscopic study[6b] of the reaction of Bu^tO_2H with Fe^{III}TDMSPP has revealed the presence of the $Bu^tO_2^\bullet$ radical in the reaction mixture and we concluded that the main route to this species is from the oxidation of Bu^tO_2H by the iron(IV) porphyrin [reaction (8)]. A preliminary ESR study with Fe^{III}T4MPyP has shown that this porphyrin also generates the $Bu^tO_2^\bullet$ radical from Bu^tO_2H.

$$Bu^tO_2H + OFe^{IV}P \longrightarrow Bu^tO_2^\bullet + Fe^{III}P \quad (8)$$

The chemistry of peroxyl radicals in solution has been extensively studied[21] and their reactions with iron(III) porphyrins have also been examined.[22] The most likely routes leading to the removal of $Bu^tO_2^\bullet$ radicals in the systems investigated here are the self-reactions, reactions (9) and (10). Although there are two alternative self-reactions, in this study as we observed previously,[6a] the trace quantities of di-t-butyl peroxide in the products implies that only the path to form $Bu^tO^\bullet$ radicals and dioxygen is important in aqueous solution.

$$2Bu^tO_2^\bullet \longrightarrow Bu^tO_4Bu^t \begin{cases} \longrightarrow Bu^tO_2Bu^t + O_2 & (9) \\ \longrightarrow 2Bu^tO^\bullet + O_2 & (10) \end{cases}$$

The formation of significant quantities of Bu^tO_2Me at first seems to contradict the conclusion above and suggests a crossed reaction between $MeO_2^\bullet$ and $Bu^tO_2^\bullet$ radicals [reaction (12)], the former species being formed by the rapid reaction of the methyl radical with dioxygen [reaction (11)]. However, it is hard to justify this route to Bu^tO_2Me when only trace quantities of di-t-butyl peroxide are formed. It should also be noted that peroxyl radicals with α-hydrogens can undergo disproportionation [reactions (13) and (15)] and these reactions should compete with reaction (12) and should further reduce the extent of mixed peroxide formation from two peroxyl radicals. That reaction (12) is not the source of t-butyl methyl peroxide is confirmed by comparison of the product yields from the reactions carried out in air and under nitrogen. Changing to the latter conditions should greatly reduce the importance of reaction (11) and consequently the yield of the mixed peroxide. However, the result is quite the contrary; the yield of t-butyl methyl peroxide increases. For these reasons we propose reaction (14) as the main source of the mixed peroxide. Thus, under nitrogen, reaction (11) is unimportant and the competitive reaction pathway, reaction (14), leading to the mixed peroxide becomes dominant. The trapping of methyl radicals by $Bu^tO_2^\bullet$ radicals is analogous to the formation of 3-cyclohexenyl t-butyl peroxide by reaction between cyclohexenyl and $Bu^tO_2^\bullet$ radicals in the cobalt(II)-catalysed oxidation of cyclohexene by t-butyl hydroperoxide.[23]

$$Me^\bullet + O_2 \longrightarrow MeO_2^\bullet \quad (11)$$

$$MeO_2^\bullet + Bu^tO_2^\bullet \longrightarrow MeO_2Bu^t + O_2 \quad (12)$$

$$MeO_2^\bullet + Bu^tO_2^\bullet \longrightarrow HCHO + Bu^tOH + O_2 \quad (13)$$

$$Me^\bullet + Bu^tO_2^\bullet \longrightarrow MeO_2Bu^t \quad (14)$$

$$MeO_2^\bullet + MeO_2^\bullet \longrightarrow MeOH + HCHO + O_2 \quad (15)$$

The Origin of Formaldehyde.—The further oxidation of methanol by the Fe^{III}T4MPyP–Bu^tO_2H system is ruled out as the major route to formaldehyde by comparing the product distributions for reactions in the presence and absence of air. Thus, low yields of formaldehyde are obtained when methanol

yields are high and *vice versa*. Instead these results strongly implicate dioxygen as the oxidant, since under nitrogen the yield of formaldehyde is very small whilst in stirred reactions in air it is the major one-carbon product.

We can rule out the reaction of methyl radicals with dioxygen [reaction (11)] followed by the disproportionation of methyl peroxyl radicals [reactions (13) and (15)] as being the major pathway to formaldehyde. This predicts that the yield of formaldehyde should equal the sum of the yields of methanol and t-butyl alcohol. Allowing for other routes to the alcohols, *e.g.* reactions (5) and (6), the yield of formaldehyde should be $\leqslant$ to the sum of the yields of methanol and t-butyl alcohol. However, stirred reactions of Bu^tO_2H with $Fe^{III}T4MPyP$ in air give >2.5 times more formaldehyde than alcohols.

We propose that the formaldehyde is formed from a methylperoxyiron porphyrin by the heterolytic elimination mechanism recently proposed by Balch and co-workers [reaction (16)].[24b] The methylperoxyiron porphyrin would arise from the reaction of methyl radicals, dioxygen and iron(II) porphyrin. However, the precise order in which these species react remains unclear. Thus, the initial step could be the very rapid reactions of methyl radical with iron(II) porphyrin[17] [reaction (17)] or dioxygen with the methyl radical [reaction (11)][25] or with iron(II) porphyrin [reaction (18)].[26] These would be followed by reactions (19),[24] (20)[22] and (21), respectively.

$$MeO_2Fe^{III}P \longrightarrow HCHO + Fe^{III}P \quad (16)$$

$$Me^{\bullet} + Fe^{II}P \longrightarrow MeFe^{III}P \quad (17)$$

$$O_2 + Fe^{II}P \longrightarrow {}^{\bullet}O_2Fe^{III}P \quad (18)$$

$$MeFe^{III}P + O_2 \longrightarrow MeO_2Fe^{III}P \quad (19)$$

$$MeO_2^{\bullet} + Fe^{II}P \longrightarrow MeO_2Fe^{III}P \quad (20)$$

$$Me^{\bullet} + {}^{\bullet}O_2Fe^{III}P \longrightarrow MeO_2Fe^{III}P \quad (21)$$

The Reactions of the Methyl Radicals.—The product studies show that the methyl radicals from reaction (4) react to form the three major products, methanol, formaldehyde and t-butylmethyl peroxide and trace quantities of methane and ethane. Which of the three major products is dominant depends on the reaction conditions. Under nitrogen, where the dioxygen content of the reaction mixture is very low, methanol and t-butyl methyl peroxide from reactions (5) and (6) and reaction (14), respectively, account for 95% of the methyl radicals and oxidation of the methyl radicals to formaldehyde is a minor pathway. In air, and more obviously in stirred reactions in air, dioxygen competes effectively for the methyl radicals leading to formaldehyde. Under the latter conditions formaldehyde accounts for 67% of the products from the methyl radicals.

The influence of dioxygen on the yields of acetone and t-butyl alcohol also arises from the trapping of methyl radicals by dioxygen [reaction (11)]. Under nitrogen this reaction is relatively unimportant and the methyl radicals are largely consumed in the competitive processes leading to increased yields of methanol and t-butyl methyl peroxide [reactions (5), (6) and (14)]. The increase in the yield of the mixed peroxide results in a decrease in availability of t-butyl peroxyl radicals for self-reaction to give t-butoxyl radicals [reaction (10)] and consequently to a reduction in the yields of t-butyl alcohol and acetone.

It is the very low yield of t-butyl alcohol in reactions carried out under nitrogen that is the most significant feature of the product distribution. This points strongly to the reactions studied here involving a homolytic cleavage of the O–O bond by $Fe^{III}T4MPyP$ [reaction (2)] and cannot readily be accommodated by a heterolytic cleavage of Bu^tO_2H [reaction (1)]. The two-electron reduction of the hydroperoxide would lead to t-butyl alcohol directly so that, unless this reaction is only important in the initial stages of the reaction, the alcohol should be a major product of reactions under nitrogen.

The yields of methane and ethane are always low and even under nitrogen they only account for 0.6% of the oxidant. However, with stirred reactions in air, where dioxygen can trap the methyl radicals, these products are present in trace amounts. The most obvious routes to these hydrocarbons is by hydrogen atom abstraction and dimerisation of the methyl radicals. The source of the hydrogen atoms is most probably the oxidant, Bu^tO_2H, and increasing its concentration leads to an expected increase in the yield of methane at the expense of ethane. Bond energy considerations would predict that the hydrogen atoms would come from the O–H rather than the C–H bonds of the Bu^tO_2H. The formation of monodeuteriomethane and the kinetic isotope effect leading to the preferential formation of ethane in reactions of Bu^tO_2D are in agreement with this conclusion.

The Role of Dioxygen.—From the discussions above it is clear that dioxygen plays an important role in the reaction of $Fe^{III}T4MPyP$ with Bu^tO_2H. It traps and oxidises methyl radicals, methyliron(III) porphyrin and iron(II) porphyrin species. However, even in anaerobic reactions some dioxygen will be formed from the peroxyl radicals, [reaction (10)]. From our previous studies using an oxygen electrode we showed that the reaction of Bu^tO_2H with $Fe^{III}TDMSPP$ does not lead to detectable amounts of dioxygen.[6a] Indeed, on the contrary, it is known that iron(III) porphyrin–Bu^tO_2H reactions result in an overall uptake of dioxygen.[27] From this we must conclude that all the dioxygen formed *in situ* under anaerobic conditions is rapidly consumed by reactions (11), (18) and (19).

The Iron Porphyrin Species Present in the Reactions of Bu^tO_2H *with* $Fe^{III}T4MPyP$ *and the Cycling of the Catalyst.*—The addition of Bu^tO_2H to aerated solutions of $Fe^{III}T4MPyP$ in water generates the red oxoiron(IV) tetra(4-*N*-methylpyridyl)-porphyrin (Fig. 8). This peroxidase compound **II** model has also been prepared from $Fe^{III}T4MPyP$ using other chemical oxidants[28] (PhIO, 3-chloroperbenzoic acid or potassium monoperoxysulphate) and by electrochemical oxidation[29] and its structure has been determined by resonance Raman, UV–VIS and ^1H NMR spectroscopy.[28b]

The oxoiron(IV) porphyrin is the dominant porphyrin species in the Bu^tO_2H–$Fe^{III}T4MPyP$ reaction mixtures in air. With >1 equiv. of oxidant there is an almost quantitative conversion of $Fe^{III}T4MPyP$ into $OFe^{IV}T4MPyP$.

There are a number of routes leading to the reduction of the initially formed oxoiron(IV) porphyrin. These include reaction with Bu^tO_2H [reaction (8)], oxidation of methyl radicals [reaction (6)] and comproportionation with iron(II) porphyrin species [reaction (22)]. The relative importance of these three reactions is dependent upon their individual rate constants and the concentrations of the Bu^tO_2H, methyl radicals and iron(II) porphyrins, respectively.

$$OFe^{IV}P + Fe^{II}P \longrightarrow 2\,Fe^{III}P \quad (22)$$

$${}^{\bullet}O_2Fe^{III}P + Fe^{II}P \longrightarrow Fe^{III}PO_2Fe^{III}P \longrightarrow 2\,OFe^{IV}P \quad (23)$$

Once the reaction is underway, other oxidising species will compete with Bu^tO_2H for the iron(II) and iron(III) porphyrins to regenerate the oxoiron(IV) species. Thus dioxygen will oxidise $Fe^{II}T4MPyP$ [reaction (18) followed by (23)] and methyl peroxyl radicals both $Fe^{II}T4MPyP$ [reaction (20)] and $Fe^{III}T4MPyP$. Under nitrogen, however, with a small excess of

Bu^tO_2H, the concentration of dioxygen in the reaction will be very low and the autoxidation of iron(II) species and the trapping of methyl radicals as methyl peroxyl radicals [reaction (11)] will be unimportant. Under these conditions, the balance of the porphyrin species could shift from oxoiron(IV) to iron(III) being the dominant species. This would explain the relatively low conversion of Fe^{III}T4MPyP into OFe^{IV}T4MPyP in these reactions. We could not detect Fe^{II}T4MPyP in reactions under nitrogen by UV–VIS spectroscopy. Presumably the iron(II) species is rapidly removed by comproportionation with the oxoiron(IV) porphyrin [reaction (22)]. With added carbon monoxide, however, the iron(II) porphyrin is stabilised and in time all the catalyst is effectively converted into $(CO)Fe^{II}$T4MPyP. In our previous study of the reaction of Fe^{III}TDMSPP with Bu^tO_2H under nitrogen it was also possible to trap the iron(II) porphyrin as its CO complex.[6b] However, the 10% yield then obtained is significantly less than in the present study.

In conclusion, the present study produces further evidence that the initial reaction of high-spin iron(III) porphyrins with t-butyl hydroperoxide generates an oxoiron(IV) species and a t-butoxyl radical. Following this initial homolysis of the O–O bond, the t-butoxyl radical fragments to acetone and a range of products derived from the methyl radical. The iron porphyrin is cycled by redox reactions involving alkyl peroxyl, and alkyl radicals, dioxygen and hydroperoxide.

Experimental

Materials.—All materials were commercially available unless otherwise stated. The aqueous t-butyl hydroperoxide was 70% w/w by iodimetric titration.[30]

t-Butyl methyl peroxide was prepared and purified following the method of Rust *et al.*[31] and was found to be 98% pure by GC analysis, *m/z* 104 (M^+ 44%), 59 (78), 58 (72), 57 (100), 43 (80), 41 (92), 31 (87), 30 (46) and 29 (96); $\delta_H[(CD_3)_2CO)]$, 1.2 (s, 9 H) and 3.7 (s, 3 H); $\delta_C[(CD_3)_2CO)]$, (couplings in off-resonance spectrum) 26.4 (q), 63.0 (q) and 80.1 (s).

t-Butyl deuterioperoxide was prepared following the method of Seubold *et al.*[32] by shaking the Bu^tO_2H (0.6 cm^3) with D_2O (99.8%, 4.15 cm^3) and allowing the solution to stand for 24 h at 4 °C. This procedure is reported to lead to 63 ± 1% deuteriation.[32]

5,10,15,20-Tetra(*N*-methyl-4-pyridyl)porphyrin was prepared using the method of Kim, Leonard and Longo[33] and was metallated with iron(II) chloride using the method of Adler *et al.*[34] The *N*-methylated derivative was obtained using methyltoluene-4-sulphonate and precipitated as its perchlorate following the procedure of Hambright *et al.* for methylation of the unmetallated tetra(4-pyridyl)porphyrin.[35] The perchlorate salt was converted into the water soluble chloride by slurrying with excess of Amberlite CG-400 (Cl^- form) in water and then passing the solution down a short Amberlite CG-400 (Cl^- form) column. The final stage of purification was by ion exchange chromatography on Amberlite CG-50 (H^+ form) with 1 mol dm^{-3} hydrochloric acid. The eluted solution of iron(III) porphyrin in aqueous acid was concentrated to dryness using a rotary evaporator and a cool water bath. The solid residue was dissolved in methanol and precipitated with chloroform. A typical sample of 5,10,15,20-tetra(*N*-methyl-4-pyridyl)porphinatoiron(III) pentachloride prepared as described above had $\lambda_{max}(H_2O$, pH 7.02) 338, 424 (ε = 10 000 m^2 mol^{-1}, lit.,[15a] 8990 m^2 mol^{-1}), 506, 596 and 635 nm, $\delta_H(CD_3OD)$ 80.5 (br s, 8 H), 13.15 (s, 8 H), 11.9 (s, 8 H) and 6.75 (s, 12 H) (Found: C, 50.9; H, 4.50; N, 10.55; Fe, 5.6. $C_{44}H_{36}N_8FeCl_5 \cdot 7H_2O$ requires C, 51.00; H, 4.83; N, 10.82; Fe, 5.41%).

Methods.—GC used a Pye-Unicam PU4500 chromatograph equipped with a flame ionisation detector. The results were analysed using a Trivector Scientific Ltd Trilab 2000 chromatography data collection system. The separation of products in aqueous solution was achieved by on-column injection with a capillary column (SGE, QC3/BP-1, 25 × 0.32 mm i.d.) at 34 °C. The hydrocarbon gases were analysed on columns packed with silica gel. GC–MS was carried out with Kratos MS3074 and MS80 spectrometers.

UV–VIS spectra were recorded on Perkin-Elmer 554 and Lambda 15 scanning spectrometers and on a Hewlett Packard 8452A diode array spectrometer. Kinetic studies were carried out on the first of these spectrometers. ^1H and ^{13}C NMR spectra were measured on a JEOL FX90Q (90 MHz) spectrometer.

pH Measurements were made with a Philips PW9410 pH meter equipped with a Russells CE7L combined pH/reference electrode.

Kinetic Procedures.—Stock solutions of Fe^{III}T4MPyP (3×10^{-5} mol dm^{-3}) were prepared in the appropriate buffer and allowed to stand for at least 24 h before use. All reactions were carried out at 30 °C in 1 cm pathlength quartz cuvettes. Reactions were initiated by adding the t-butyl hydroperoxide solution to a buffered solution of Fe^{III}T4MPyP, ABTS and sodium nitrate (sufficient to obtain an ionic strength of 0.20 mol dm^{-3}) and had a total volume of 3 cm^3. The pH of the reaction mixtures was measured before the addition of the Bu^tO_2H and checked not to have changed by more than ±0.04 pH units at the end of the reaction.

The kinetics of the reactions were followed by monitoring the increase in absorbance of $ABTS^{\bullet+}$ at 660 nm. The values of log A_{660} *vs.* time were used to obtain pseudo-first-order rate constants using an Apple II computer.

Product Studies.—In a typical reaction, Bu^tO_2H (to make an initial concentration of 2.5×10^{-3} mol dm^{-3}) was added to Fe^{III}T4MPyP (5.0×10^{-6} mol dm^{-3}) and ABTS (0.03 mol dm^{-3}) in 0.1 mol dm^{-3} borate buffer solution (3 cm^3, pH 9.2) with an ionic strength 0.20 mol dm^{-3} ($NaNO_3$). The reaction was thoroughly shaken and left to stand for 1.5 h before the products in the aqueous solution were analysed.

For the anaerobic reactions, all the reagent solutions were thoroughly deoxygenated with nitrogen gas and the reaction flask was sealed with a Teflon tap. The use of a Suba-seal to stopper the reaction flask led to poor product balances, possibly through absorption of some products into the rubber seal.

The gaseous hydrocarbon products were analysed by GC and GC–MS by removing samples of the headspaces gases from sealed reaction mixtures using a gas-tight syringe.

Carbon Monoxide Trapping of Fe^{II}T4MPyP.—A 5×10^{-6} mol dm^{-3} solution of Fe^{III}T4MPyP in 0.1 mol dm^{-3} borate buffer (pH 9.2) was sealed in a cuvette with a Suba-seal and thoroughly deaerated with nitrogen gas before being saturated with carbon monoxide. The Bu^tO_2H (5×10^{-5} mol dm^{-3}, deaerated with nitrogen) was added and the UV–VIS spectrum was measured immediately after mixing and at selected times during the following 12 h, using the diode array spectrometer. The concentrations of Fe^{III}T4MPyP, OFe^{IV}T4MPyP and $(CO)Fe^{II}$T4MPyP at different times in the reaction were obtained by fitting the UV–VIS spectra of the reaction mixture with the Hewlett Packard HP89511A Quant II software using standard spectra of each of the three species.

The standard spectrum of OFe^{IV}T4MPyP was obtained by adding a tenfold excess of Bu^tO_2H to 5×10^{-6} mol dm^{-3} Fe^{III}T4MPyP in 0.1 mol dm^{-3} borate buffer (pH 9.2) under aerobic conditions and had λ_{max} = 427 nm, ε_{max} = 12 500 m^2 mol^{-1}. The $(CO)Fe^{II}$T4MPyP was prepared by adding a deaerated solution of 1.2 mol dm^{-3} sodium dithionite (0.01 cm^3) to

a carbon monoxide saturated 5×10^{-6} mol dm^{-3} solution of $Fe^{III}T4MPyP$ (3 cm^3) and had λ_{max} = 426 nm, ε_{max} = 15 400 m^2 mol^{-1}.

Acknowledgements

One of us (R. I. L.) thanks the SERC and Unilever Research for a CASE Research Studentship.

References

1 H. B. Dunford and J. S. Stillman, *Coord. Chem. Rev.*, 1976, **19**, 187.
2 G. R. Schonbaum and B. Chance, in *The Enzymes*, ed. P. D. Boyer, Acad. Press, New York, 3rd edn., 1973, vol. 8C, p. 363.
3 E. G. Hrycay and P. J. O'Brien, *Arch. Biochem. Biophys.*, 1971, **147**, 4; 1973, **157**, 7 and 1974, **160**, 230; K. C. Kadlubar, K. C. Morton, and D. M. Ziegler, *Biochem. Biophys. Res. Commun.*, 1973, **54**, 1255; G. D. Nordblom, R. E. White and M. J. Coon, *Arch. Biochem. Biophys.*, 1976, **175**, 524; R. C. Blake and M. J. Coon, *J. Biol. Chem.*, 1981, **256**, 12127; M. B. McCarthy and R. E. White, *J. Biol. Chem.*, 1983, **258**, 9135.
4 G. Plaa and H. Witschi, *Annu. Rev. Pharmacol.*, 1976, **16**, 125; B. Chance, H. Sies and H. Boveries, *Physiol. Rev.*, 1979, **59**, 527.
5 T. G. Traylor, W.-P. Fann and D. Bandyopadhyay, *J. Am. Chem. Soc.*, 1989, **111**, 8009; T. G. Traylor and F. Xu, *J. Am. Chem. Soc.*, 1990, **112**, 178 and earlier papers.
6 *a* J. R. Lindsay Smith, P. N. Balasubramanian and T. C. Bruice, *J. Am. Chem. Soc.*, 1988, **110**, 7411; *b* P. N. Balasubramanian, J. R. Lindsay Smith, M. J. Davies, T. W. Kaaret and T. C. Bruice, *J. Am. Chem. Soc.*, 1989, **111**, 1477.
7 R. D. Arasasingham, C. R. Cornman and A. L. Balch, *J. Am. Chem. Soc.*, 1989, **111**, 7800.
8 D. Mansuy, J.-F. Bartoli and M. Momenteau, *Tetrahedron Lett.*, 1982, **23**, 2781; J. R. Lindsay Smith and D. N. Mortimer, *J. Chem. Soc., Perkin Trans. 2*, 1986, 1743.
9 R. Labeque and L. J. Marnett, *J. Am. Chem. Soc.*, 1989, **111**, 6621.
10 D. Mansuy, P. Battioni and J.-P. Renaud, *J. Chem. Soc., Chem. Commun.*, 1984, 1255; J.-P. Renaud, P. Battioni, J. F. Bartoli and D. Mansuy, *J. Chem. Soc., Chem. Commun.*, 1985, 888.
11 J. T. Groves, R. C. Haushalter, M. Nakamura, T. E. Nemo and B. J. Evans, *J. Am. Chem. Soc.*, 1981, **103**, 2884; W. A. Lee and T. C. Bruice, *J. Am. Chem. Soc.*, 1985, **107**, 513; S. Hashimoto, Y. Tatsumo and T. Kitagawa, *J. Am. Chem. Soc.*, 1987, **109**, 8096; H. Sugimoto, H.-C. Tung, and D. T. Sawyer, *J. Am. Chem. Soc.*, 1988, **110**, 2465; A. Gold, K. Jayaraj, P. Doppelt, R. Weiss, G. Chottard, E. Bill, X. Ding and A. X. Trautwein, *J. Am. Chem. Soc.*, 1988, **110**, 5756; T. C. Bruice, P. N. Balasubramanian, R. W. Lee, and J. R. Lindsay Smith, *J. Am. Chem. Soc.*, 1988, **110**, 7890.
12 M. F. Zipplies, W. A. Lee and T. C. Bruice, *J. Am. Chem. Soc.*, 1986, **108**, 4433.
13 T. Nash, *J. Biochem.*, 1953, **55**, 416.
14 (*a*) E. B. Fleischer, J. M. Palmer, T. S. Srivastava and A. J. Chatterjee, *J. Am. Chem. Soc.*, 1971, **93**, 3162; (*b*) H. Goff and L. O. Morgan, *Inorg. Chem.*, 1976, **15**, 3180; (*c*) A. El-Awady, P. C. Wilkins and R. G. Wilkins, *Inorg. Chem.*, 1985, **24**, 2053.
15 (*a*) F. L. Harris and D. L. Toppen, *Inorg. Chem.*, 1978, **17**, 71; (*b*) N. Kobayashi, M. Koshiyama, T. Osa and T. Kuwana, *Inorg. Chem.*, 1983, **22**, 3608; (*c*) G. A. Tondreau and R. G. Wilkins, *Inorg. Chem.*, 1986, **25**, 2745; (*d*) G. M. Miskelly, W. S. Webley, C. R. Clark and D. A. Buckingham, *Inorg. Chem.*, 1988, **27**, 3773; (*e*) S. E. J. Bell, J. N. Hill, R. E. Hester, D. R. Shawcross and J. R. Lindsay Smith submitted to *J. Chem. Soc., Faraday Trans.*, 1990, issue 24.
16 M. Erban-Russ, C. Michel, W. Bors and M. Saran, *J. Phys. Chem.*, 1987, **91**, 2362.
17 D. Brault and P. Neta, *J. Am. Chem. Soc.*, 1981, **103**, 2705.
18 J. T. Groves and G. A. McClusky, *J. Am. Chem. Soc.*, 1976, **98**, 859.
19 P. R. Ortiz de Montellano and R. A. Stearns, *J. Am. Chem. Soc.*, 1987, **109**, 3415.
20 T. G. Traylor and F. Xu, *J. Am. Chem. Soc.*, 1987, **109**, 6201.
21 J. A. Howard, *Adv. Free Radical Chem.*, 1972, **4**, 55.
22 D. Brault and P. Neta, *J. Phys. Chem.*, 1984, **88**, 2857.
23 J. D. Koola and J. K. Kochi, *J. Org. Chem.*, 1987, **52**, 4545.
24 (*a*) R. D. Arasasingham, A. L. Balch and L. Latos-Grazynski, *J. Am. Chem. Soc.*, 1987, **109**, 5846; (*b*) R. D. Arasasingham, A. L. Balch, C. R. Cornman and L. Latos-Grazynski, *J. Am. Chem.*, 1989, **111**, 4357.
25 C. J. Hochanadel, J. A. Ghormley, J. W. Boyle and P. J. Ogren, *J. Phys. Chem.*, 1977, **81**, 3.
26 D. H. Chin, A. L. Balch and G. N. La Mar, *J. Am. Chem. Soc.*, 1980, **102**, 1446; A. L. Balch, Y.-W. Chan, R.-J. Cheng, G. N. La Mar, L. Latos-Grazynski and M. W. Renner, *J. Am. Chem. Soc.*, 1984, **106**, 7779.
27 B. Kalyamaraman, C. Mottley and R. P. Mason, *J. Biol. Chem.*, 1983, **258**, 3855.
28 S. E. J. Bell, R. E. Hester and J. R. Lindsay Smith, in *Proceedings of the Fourth International Conference on Time-resolved Vibrational Spectroscopy*, ed. T. G. Spiro, Princeton, New Jersey, 1989, p. 29; S. E. J. Bell, P. R. Cooke, P. Inchley, D. R. Leanord, J. R. Lindsay Smith, R. J. Lower and A. Robbins, Poster presentation at the European Conference on Homogeneous Catalysis, Arles, France, September 1989.
29 S.-M. Chen and Y. O. Su, *J. Chem. Soc., Chem. Commun.*, 1990, 491.
30 A. I. Vogel, in *Textbook of Quantitative Inorganic Analysis*, Longmans, London, 3rd edn., 1961, p. 363.
31 F. F. Rust, F. H. Seubold and W. E. Vaughan, *J. Am. Chem. Soc.*, 1950, **72**, 338.
32 F. H. Seubold, F. F. Rust and W. E. Vaughan, *J. Am. Chem. Soc.*, 1951, **73**, 18.
33 J. R. Kim, J. J. Leonard and F. R. Longo, *J. Am. Chem. Soc.*, 1972, **94**, 3986.
34 A. D. Adler, F. R. Longo, F. Kampas and J. Kim, *J. Inorg. Nucl. Chem.*, 1970, **32**, 2443.
35 P. Hambright, A. Adeyeme, A. Shaimim and S. Levielle, *Inorg. Synth.*, 1985, **23**, 55.

Paper 0/03268I
Received 23*rd July* 1990
Accepted 30*th August* 1990